KEY FACTORS THAT INFLUENCE THE PERFORMANCE PROPERTIES OFARP/MCU SALTSTONE MIXES

J. R. Harbour, T. B. Edwards and V. J. Williams

Savannah River National Laboratory

September 2009

DISCLAIMER

Printed in the United States of America

Prepared For
U.S. Department of Energy

KEY FACTORS THAT INFLUENCE THE PERFORMANCE PROPERTIES OFARP/MCU SALTSTONE MIXES

J. R. Harbour, T. B. Edwards and V. J. Williams

Savannah River National Laboratory

September 2009

REVIEWS AND APPROVALS

AUTHORS:

_____
J. R. Harbour, SRNL, Engineering Process Development   Date

_____
T. B. Edwards, SRNL, Applied Comp Eng & Statistics   Date

_____
V. J. Williams, SRNL, Engineering Process Development   Date

TECHNICAL REVIEWERS:

_____
M. M. Reigel, SRNL, Engineering Process Development   Date

APPROVERS

_____
A. B. Barnes, SRNL, Manager, Engineering Process Development   Date

_____
S. L. Marra, SRNL, Manager, E&CPT Research Programs   Date

_____
J. E. Occhipinti, Manager, Waste Solidification Engineering   Date

EXECUTIVE SUMMARY

This report details the results from Task 3 of the Saltstone Variability Study for FY09 which was performed to identify and quantify, when possible, those factors that drive the performance properties of the projected Actinide Removal Process/ Modulated Caustic Side Solvent (ARP/MCU) Batches. A baseline ARP/MCU mix (at 0.60 w/cm ratio) was established and consisted of the normal premix composition and a salt solution that was an average of the projected compositions of the last three ARP/MCU batches developed by T. A. Le. The strategy for this task introduced significant variation in (1) wt % slag, w/cm ratio, and wt % portland cement about the baseline mix and (2) the temperature of curing in order to better assess the dependence of the performance properties on these factors.

The baseline salt solution contained the projected value of 0.22 M aluminate which was held constant for all mixes except one. The exception was a mix batched with a salt solution containing 0.05 M aluminate (previous baseline) but equivalent to the baseline salt solution in all other constituents. The relatively high 0.22 M aluminate concentration (compared with the 0.05 M aluminate mix) in the projected ARP/MCU batches more than doubled Young's modulus from 4.2 to 8.8 GPa. Therefore, the higher concentration of aluminate in the new baseline salt solution significantly improved performance for mixes cured at 22 °C.

For samples cured at 22 °C, a decrease in the w/cm ratio from 0.65 to 0.50 in these mixes increased Young's modulus and decreased total porosity. An increase in the wt % slag from 45 to 60 wt % also increased Young's modulus and reduced total porosity. This is consistent with previous findings and leads to the conclusion that w/cm ratio and slag content are important factors that drive the performance properties.

For samples cured at 22 °C, an increase in the cement content in the premix from 10 to 30 wt % decreased E from 8.8 to 7.2 GPa. This effect is opposite to that of increased slag concentration in the premix. However, this result is consistent with literature findings that show slag produces mixes that have lower permeabilities and porosities. For cement content of 15 or 30 wt % in the premix, a decrease in w/cm ratio increased Young's modulus and decreased total porosity.

Linear, empirical models were developed and are presented in this report for Young's modulus, total porosity and heat of hydration using data from the 22 °C cured samples. The R^2 values for these three models ranged from 92 % to 99 % and identified the statistically significant factors that influenced these properties for this study.

An increase in the curing temperature in general reduced Young's modulus and increased total porosity. For example the baseline mix cured at 54 °C had a Young's modulus value roughly half the value of the sample cured at 22 °C. This reduction in performance properties for samples cured at higher temperatures is mitigated by an increase in the cement content of the premix. For a mix containing 30 wt % cement (at the expense of fly ash), the value of Young's modulus was essentially equivalent for samples cured at 60 °C and 22 °C.

For the mixes containing variable slag concentration, the processing properties were generally acceptable except for those mixes at the lowest w/cm ratios. The measured gel times for these

mixes were 10 minutes and the viscosities and yield strengths were higher than normal. Similar results were found for mixes containing high levels of cement. These mixes exhibited short gel times and increased viscosities and yield strengths.

Samples from these tests were dried at 40 °C until they had lost ~ 20 wt % due to water evaporation. When these dried samples were broken apart, the smaller pieces that resulted had many surfaces indicating cleavage along internal cracks. This behavior was observed with all samples containing 0.22 M aluminate but not for the mix containing 0.05 M aluminate. In the 0.05 M aluminate case, there was a clean break in the cylindrical sample with the large pieces having smooth surfaces.

When partially dried samples (mass loss < 10 wt %) were broken apart, the cross sectional area consisted of distinct regions. The outer region was highly fractured whereas the inner region was blue in color, saturated and intact. A mechanism of shrinkage and subsequent cracking accounts for these observations. Evidently, the samples dry from the outside first which leads to shrinkage and then cracking of the grout. This dried and cracked region is highly permeable such that water from the inner regions escapes from the grout by passing through this porous outer region as drying continues. The kinetics of this process are such that a very sharp demarcation boundary exists between the two phases. Photographs of the dried and cracked grouts are provided in the report.

TABLE OF CONTENTS

LIST OF FIGURES

LIST OF TABLES

LIST OF ACRONYMS

ACTL	Aiken County Technology Laboratory
ARP	Actinide Removal Process
BSE	Back Scattered Electrons
CBO	Carbon Burn-Out
CSH	Calcium Silicate Hydrate
E	Young's Modulus
FA	Class F Fly Ash
BFS	Blast Furnace Slag
DSS	Decontaminated Salt Solution
GPa	Giga Pascals
GVS	Grout Variability Study
ISDP	Interim Salt Disposition Processing
M	Molarity
MCU	Modular Caustic Side Solvent Extraction
OPC	Ordinary Portland Cement
Φ	Total Porosity
PA	Performance Assessment
PC	Portland Cement
SDF	Saltstone Disposal Facility
SEM	Scanning Electron Microscopy
SPF	Saltstone Production Facility
SRNL	Savannah River National Laboratory
SRNS	Savannah River Nuclear Solutions
SRS	Savannah River Site
SWPF	Salt Waste Processing Facility
T	Temperature
TR	Trial Run
w/cm	Water to Cementitious Material Ratio
Wt	Weight

1.0 INTRODUCTION

At the Saltstone Production Facility (SPF), decontaminated salt solution (DSS) is combined with premix (a cementitious mixture of portland cement (PC), blast furnace slag (BFS) and Class F fly ash (FA)) in a Readco mixer to produce fresh (uncured) Saltstone. After transfer to the Saltstone Disposal Facility (SDF) the hydration reactions initiated during the contact of the premix and salt solution continue during the curing period to produce the hardened waste form product. The amount of heat generated from hydration and the resultant temperature increase in the vaults depend on the composition of the decontaminated salt solution being dispositioned as well as the grout formulation (mix design).

This report details the results from Task 3 of the Saltstone Variability Study for FY09 [1] which was performed to identify, and quantify when possible, those factors that drive the performance properties of the projected ARP/MCU Batches. A baseline ARP/MCU mix (at 0.60 water to cementitious materials (w/cm) ratio) was established and consisted of the normal premix composition and a salt solution that was an average of the projected compositions of the last three ARP/MCU batches developed by T. A. Le [2]. This task introduced significant variation in (1) wt % slag, w/cm ratio, and wt % portland cement about the baseline mix and (2) the temperature of curing in order to better assess the dependence of the performance properties on these factors.

Two separate campaigns, designated Phase 10 and Phase 11, were carried out under Task 3. Experimental designs and statistical analyses were used to search for correlation among properties and to develop linear models to predict property values based on factors such as w/cm ratio, slag concentration, and portland cement concentration. It turns out that the projected salt compositions contained relatively high amounts of aluminate (0.22 M) even though no aluminate was introduced due to caustic aluminate removal from High Level Waste. Previous studies revealed that increased levels of aluminate in the feed cause a significant increase in the heat generation [3]. For Phase 10, a mix with 0.05 M aluminate was used as a comparison point for the mixes at 0.22 M aluminate.

The temperature of curing in Task 3 ranged from 22°C to 75 °C. Recent results [4] demonstrated that it is not only the temperature of curing which is important but also the time/temperature sequence of curing. Therefore, this report also focuses on the impact of the sequencing of time and curing temperature on Saltstone properties.

2.0 EXPERIMENTAL

2.1 Materials

The cementitious materials were obtained from Saltstone in five gallon containers and are listed in Table 2-1. These materials were specified in a contract for Saltstone cementitious materials and arrived with the delivery of the cementitious materials to Saltstone. The materials were transferred to smaller high-density polyethylene bottles at Aiken County Technology Laboratory (ACTL) and the bottles were tightly sealed.   Maintaining these materials in a tightly sealed container limits the exposure of the materials to humid air and hydration prior to use. Table 2-1 also contains the wt% contribution of each material used to make the nominal premix. The fly ash used in this study was a material that had been thermally treated by the vendor to remove most of the carbon and ammonia (carbon burnout or CBO fly ash).

Table 2-1 Saltstone Cementitious Materials and Current Premix Blend.

Material	Category	Vendor	Premix Blend (wt%)
Portland cement (OPC)	Type II	Holcim	10
Blast Furnace slag (GGBFS)	Grade I or II	Holcim	45
Fly ash (FA)	Class F	SEFA	45

2.2 Experimental Design

The mixes prepared for this study were included in either Phase 10 or 11 of the Saltstone Variability study. The designs for both phases are presented with the results of these studies in Sections 3 and 4.

2.3 Measurement of Properties

The measurements of heat of hydration [4], dynamic Young's modulus [5], porosity [6], and processing properties such as set time [7] were performed by the methods used previously.

2.4 Curing at Higher Temperatures

Samples were cured at ambient (also referred to as room temperature in this report) conditions in the laboratory (typically 22 °C), at 40 °C or at higher temperatures (54 °C and 75 °C for Phase 10 or 60 °C for Phase 11). In all cases the grout was poured into the cylinders, capped and securely taped. Measurement of the mass of the samples with container, lid and tape were made prior to and after curing to measure any mass loss during curing. At ambient temperature and at 40 °C curing conditions, essentially no change in the mass after curing was noted. For the 54 °C and the 60 °C curing conditions, a mass loss on the order of 1 to 2 grams was observed. For example, the Young's modulus cylinder and sample have a starting mass of ~ 1100 grams. Therefore, a loss of 1 gram corresponds to only ~ 0.1 wt % of the total mass of the sample.

The ovens have temperature gradients within the interior of the ovens. Therefore, the range of temperatures for a given sample may be as great as ± 5 °C about a set temperature. Thermocouples and thermometers were used to measure the actual temperatures within the oven.

3.0 RESULTS AND DISCUSSION FOR PHASE 10

The results presented in this report were generated as part of Task 3 of the Saltstone Variability Study for FY09 and focus on the dependence of performance properties on factors such as w/cm ratio, wt % BFS, wt % PC and temperature of curing. Simulants used in this task were based on projections of the ARP/MCU batches provided by T. A. Le [2]. An experimental design was developed that used the baseline composition with variation introduced in the w/cm ratio and in the amount of BFS. An additional mix was added to the design that contained 0.05 M aluminate rather than the 0.22 M aluminate projected by Le to assess the impact of aluminate on the properties. Task 3 was comprised of Phases 10 and 11 of the Variability Study. Section 3 of this report focuses on Phase 10 of Task 3 with an experimental design as provided in Table 3-1. Phase 11 results are presented in Section 4 of this report.

Table 3-1 Experimental Design for Phase 10.

MCU Grout Variability Study Phase 10											
Run Number	Temp	Water/Premix	Water/Premix	OPC	FA	Slag	Added OH	Free OH	Nitrate plus Nitrite	Phosphate	Aluminate
Run Order	oC	Nominal	As Batched	Wt %	Wt %	Wt %	M	M	M	M	M
GVS107	22	0.60	0.605	10	45	45	2.00	1.80	2.91	0.012	0.05
GVS108	22	0.50	0.493	10	45	45	2.68	1.80	2.91	0.012	0.22
GVS109	22	0.55	0.542	10	45	45	2.68	1.80	2.91	0.012	0.22
GVS110	22	0.60	0.591	10	45	45	2.68	1.80	2.91	0.012	0.22
GVS111	22	0.65	0.640	10	45	45	2.68	1.80	2.91	0.012	0.22
GVS112	22	0.50	0.493	10	30	60	2.68	1.80	2.91	0.012	0.22
GVS113	22	0.55	0.542	10	30	60	2.68	1.80	2.91	0.012	0.22
GVS114	22	0.60	0.591	10	30	60	2.68	1.80	2.91	0.012	0.22
GVS115	22	0.65	0.640	10	30	60	2.68	1.80	2.91	0.012	0.22

3.1 Impact of Aluminate

A comparison on the impact of aluminate on the ARP/MCU mix properties was made using two mixes that were identical except for the aluminate concentration (0.05 M for GVS107 vs. 0.22 M for GVS110). Thuy Le projected that the remaining three batches of ARP/MCU will have aluminate concentrations of 0.22 M. Figure 3-1 shows the comparison of the heat of hydration as a function of time for these two mixes at 25 °C. The higher aluminate level in GVS110 leads to an induction period followed by an increased heat of hydration consistent with previous results. GVS107 was the only mix batched at the 0.05 M aluminate level for Phase 10.
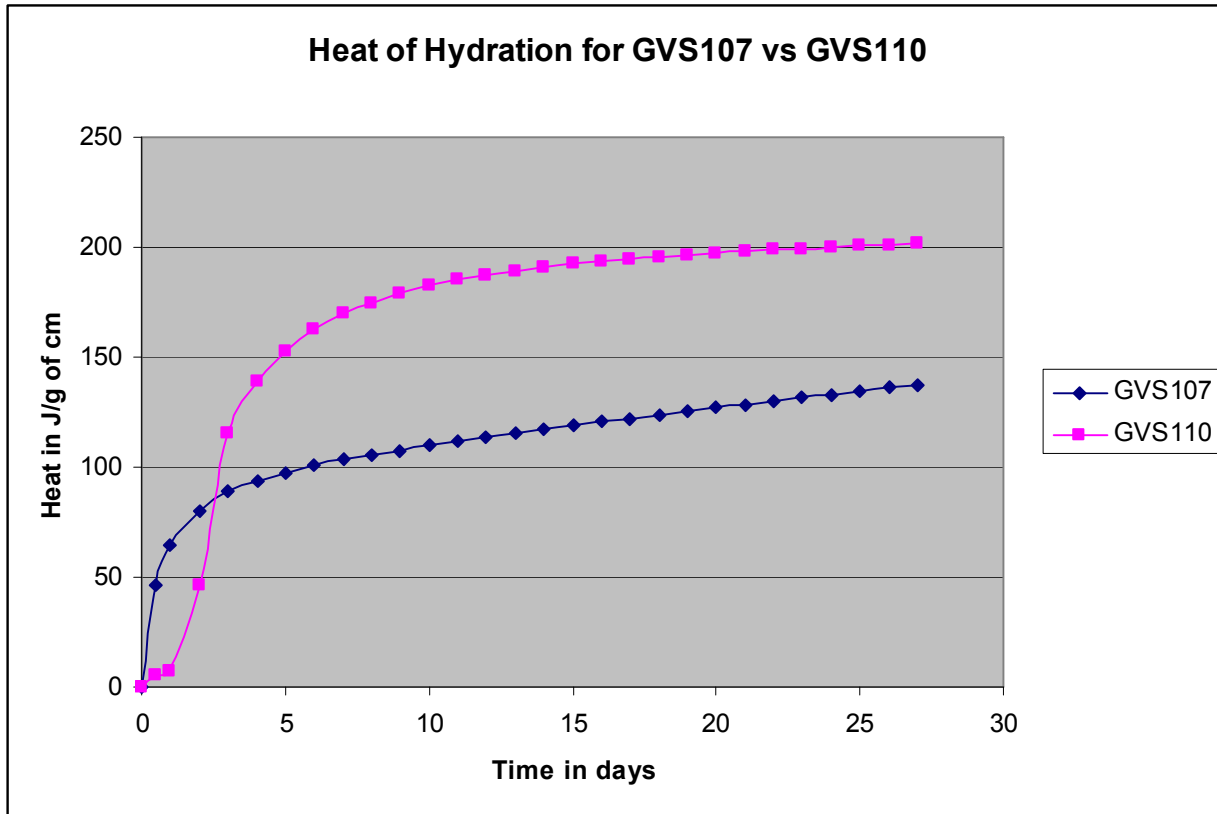
Figure 3-1 Comparison of the heat of hydration for GVS107 and GVS110.

The fresh and cured grout properties of these two mixes are presented in Table 3-2. The induction period in the heat of hydration for GVS110 is also reflected in the 3 day set time for GVS110 as compared to the 1 day set time for GVS107. The higher aluminate mix also has a Young's modulus value that is more that double the value of E for the 0.05 M aluminate mix consistent with the higher heat of hydration.

Table 3-2 Fresh and Cured Grout Properties for GVS107 and GVS110.

Identifier	Gel Time	Fresh Density	Cured Density	Flow	Yield Stress	Viscosity	Bleed	Set Time
	minutes	g/mL	g/mL	inches	Pa	cP	Vol %	Days
GVS107	30	1.717	1.753	21.4	6.2	98.4	0.0	1.0
GVS110	30	1.722	1.750	23.3	4.7	89.5	0.5	3.0

	Porosity	Heat	E
	Volume %	J/g cm	GPa
GVS107	59.1	139.0	4.2
GVS110	57.2	202.0	8.8

3.2 Phase 10 – Young's Modulus as a Function of w/cm Ratio and Wt % BFS

The values of Young's moduli for the eight ARP/MCU mixes for Phase 10 (GVS108 – GVS115) as a function of w/cm ratio at two different slag loadings are presented in Figure 3-2. These samples were cured under sealed conditions at room temperature (22 °C). It is clear from these data that decreasing the w/cm ratio from 0.65 to 0.50 increases Young's modulus by ~ 25 % independent of the slag loading. Based on literature values of Young's modulus, this increase in E can be associated with significant changes in the permeability. The second conclusion that can be drawn from these data is that an increase in wt % slag from 45 to 60 wt % in the mixes at the expense of fly ash increases Young's modulus by ~ 12 %. Therefore, by reducing the w/cm ratio and/or increasing the wt % slag content, an improvement in performance as measured by Young's modulus can be achieved for room temperature cured samples. As previously discussed, there is also an increase in Young's modulus for the samples as a result of an increase in the aluminate level from 0.05 M in the previous baseline to 0.22 M in the current baseline.
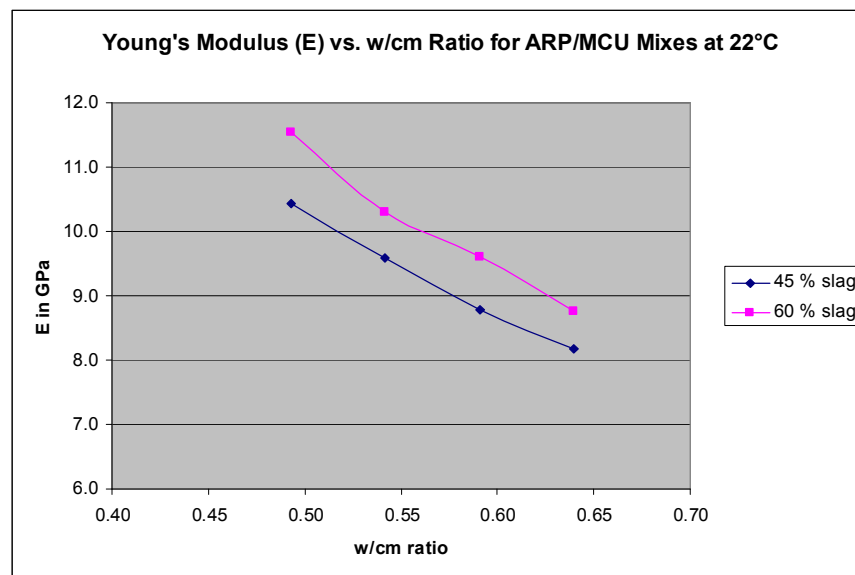
Figure 3-2 Young's modulus (E) values for eight ARP/MCU mixes as a function of w/cm ratio and wt % slag for samples cured at 22 °C.

The time dependence of Young's Modulus for the mixes cured at 22 °C is provided in Figure 3-3. These results reveal that the mixes in general continue to hydrate with time over the span of the measurements.

5
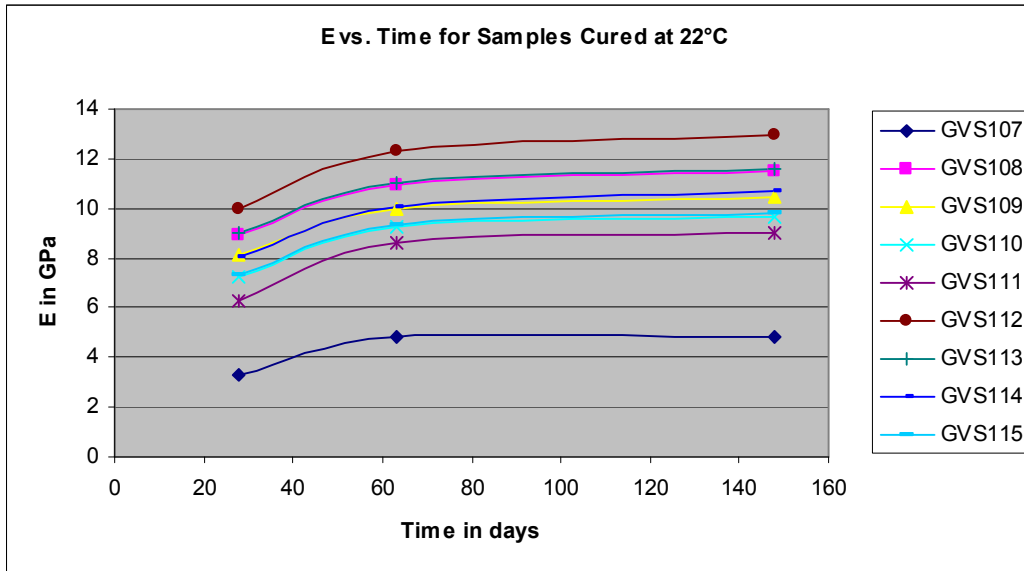
Figure 3-3 Time dependence of E for nine ARP/MCU mixes as a function of w/cm ratio and wt % slag for samples cured at 22 °C.

Samples of these mixes were also cured in sealed cylinders in ovens at 40 °C and 54 °C for 28 days to determine the impact of curing temperature on the performance properties of Saltstone. One additional sample was cured at 54 °C for 1 week, removed from the oven and then cured for the remaining 21 days at ambient temperature. The values for the 28 day Young's modulus for each of these samples at two different slag concentrations (45 wt % and 60 wt %) are provided in Figure 3-4.
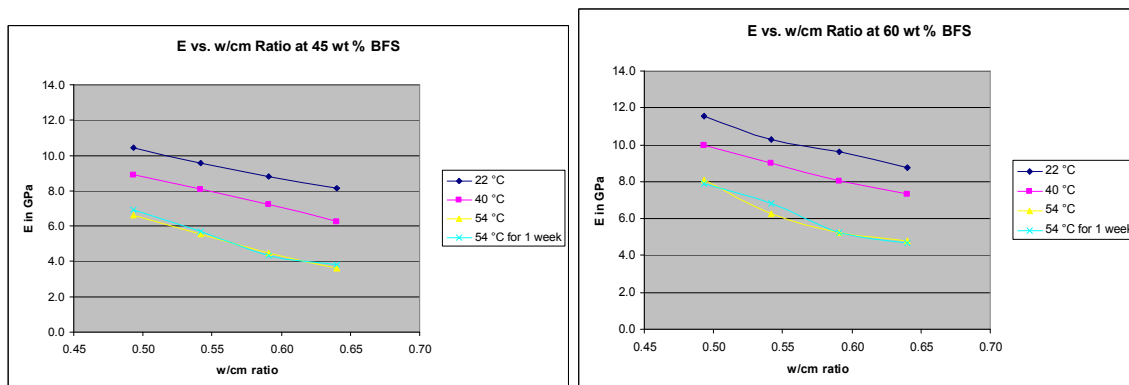
Figure 3-4 Young's modulus values for ARP/MCU mixes containing 45 or 60 wt % slag after curing at the indicated temperatures for 28 days. The data points for the cyan colored x's were obtained on the samples removed from the 54 °C oven at 1 week and measured at 28 days.

The data in Figure 3-4 reveal that E values are significantly reduced at higher curing temperatures. Furthermore, the E values for the samples initially cured at 54 °C for one week and then removed and cured at ambient temperature are essentially identical to the samples cured

for the entire 28 days at 54 °C. This implies that no further hydration reactions occurred after one week of curing at 54 °C.

The time dependence of E for Samples cured at 40 °C and 54 °C for 28 days and then removed and stored in sealed containers under ambient temperatures are provided in Figure 3-5. Unlike the samples cured at 22 °C (Figure 3-3), the hydration reactions in the samples cured at higher temperatures change very little with time.
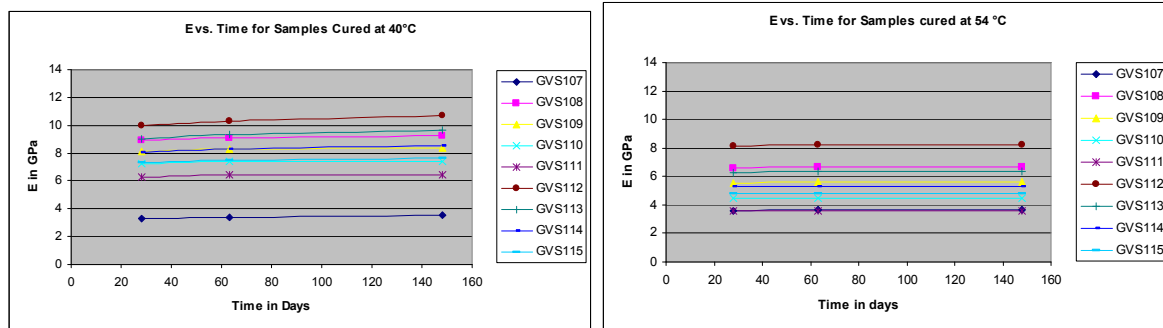
Figure 3-5 Time dependence of E for samples cured at either 40 °C or 54 °C for 28 days and then removed, sealed and stored at ambient temperature.

3.3 Young's Modulus at Different Time/Temperature Curing Profiles

Previous results [4] have shown that the performance properties of the mixes depend on the time/temperature profile for curing. Figure 3-6 shows the dependence of E on time and temperature curing profile for a mix at 0.55 w/cm ratio and 45 wt % slag (GVS109). The time/temperature curing profile for each curve is provided in the chart below the figure. The data show that an increase in temperature to 54 °C after 1 through 4 days curing at 22 °C essentially stops any further hydration. Therefore, a mix that has cured for only one day at 22 °C prior to curing at an elevated temperature does not reach as high an E value as a mix which is allowed to remain at 22 °C for 3 days. For mixes cured initially at 54 °C, removal after 1 or 2 days at 54 °C results in mixes with lower E values than the mix cured for 7 days at 54 °C. Therefore, any change in curing temperature (from 54 °C to 22 °C or from 22 °C to 54 °C) results in lower E values than achieved by curing over the entire time at one temperature.

Figure 3-7 shows the results for curing temperature profiles at 40 °C and 75 °C. The samples cured at 75 °C had the lowest values of E. Those samples cured at 40 °C had E values between the values for samples cured at 22 °C and the values for samples cured at 54 °C.
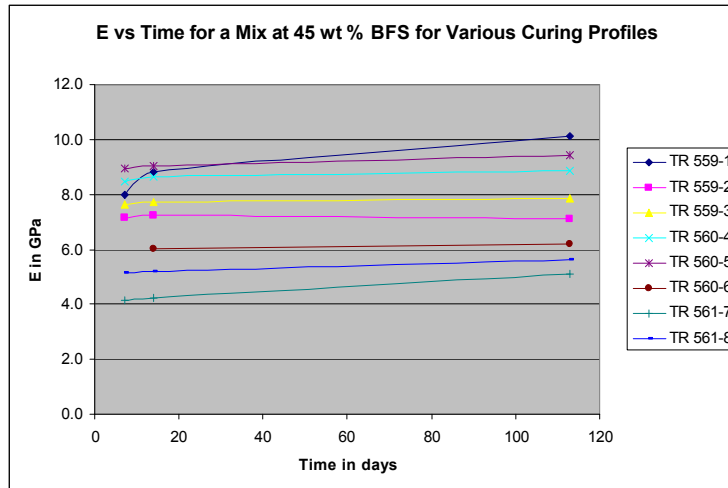
TR #	Time/ Temperature Profile	TR #	Time/ Temperature Profile
TR 559-1	Curing only at 22 °C	TR 560-5	4 days at 22 °C and 3 days at 54 °C
TR 559-2	1 day at 22 °C and 6 days at 54 °C	TR 560-6	7 days at 54 °C
TR 559-3	2 days at 22 °C and 5 days at 54 °C	TR 561-7	1 day at 54 °C and 6 days at 22 °C
TR 560-4	3 days at 22 °C and 4 days at 54 °C	TR 561-8	2 days at 54 °C and 5 days at 22 °C

Figure 3-6 Time dependence of E in GPa for GVS109 (45 wt % slag) at indicated time and temperature profiles.
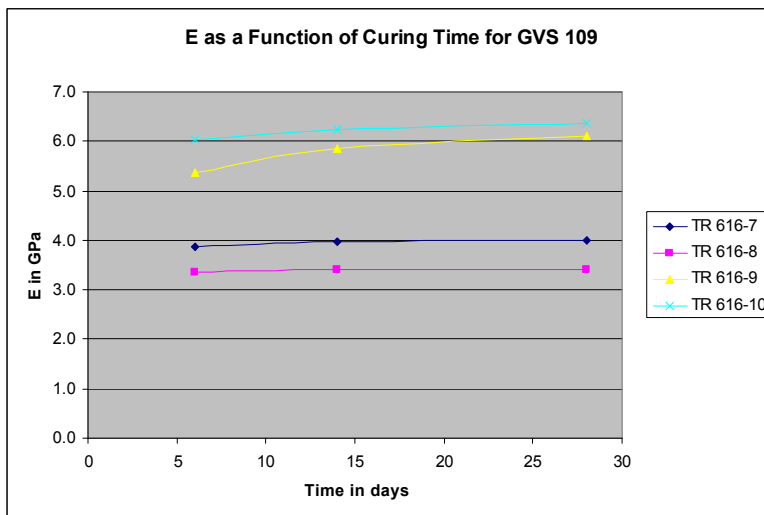
TR #	Time/ Temperature Profile
TR 616-7	7 days at 75 °C
TR 616-8	1 day at 75 °C and 6 days at 22 °C
TR 616-9	1 day at 40 °C and 6 days at 22 °C
TR 616-10	7 days at 40 °C

Figure 3-7 Time dependence of E in GPa for GVS109 (45 wt % slag) at indicated time and temperature profiles.

8

Similar results were obtained for the mixes containing 60 wt % BFS (GVS113) under the same set of time and temperature profiles (see Figure 3-8).
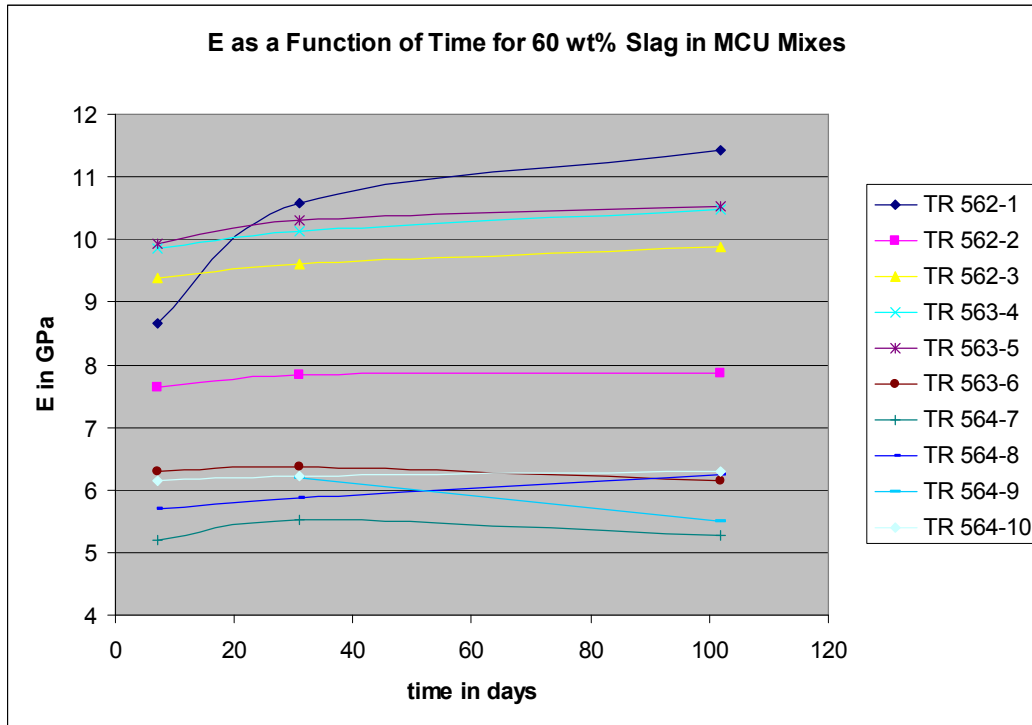
TR #	Time/ Temperature Profile	TR #	Time/ Temperature Profile
TR 562-1	Curing only at 22 °C	TR 563-6	7 days at 54 °C
TR 562-2	1 day at 22 °C and 6 days at 54 °C	TR 564-7	1 day at 54 °C and 6 days at 22 °C
TR 562-3	2 days at 22 °C and 5 days at 54 °C	TR 564-8	2 days at 54 °C and 5 days at 22 °C
TR 563-4	3 days at 22 °C and 4 days at 54 °C	TR 564-9	3 days at 54 °C and 4 days at 22 °C
TR 563-5	4 days at 22 °C and 3 days at 54 °C	TR 564-10	4 days at 54 °C and 3 days at 22 °C

Figure 3-8 Time dependence of E in GPa for GVS113 (0.55 w/cm ratio and 60 wt % slag) at indicated time and temperature profiles.

3.4 Porosities as a Function of Curing Temperature and Time

The impact of w/cm ratio and slag content on total porosity, Φ, was determined for the Phase 10 ARP/MCU mixes at 0.50, 0.55, 0.60, and 0.65 w/cm ratios for premixes containing either 45 or 60 wt % slag. The total porosity values (expressed as fractions) for samples cured at 22 °C are shown in Figure 3-9. The total porosity decreases with (1) decreasing w/cm ratio and (2) increasing slag content. This is consistent (porosity and E are inversely related [9, 10]) with the trend of Young's Modulus values for these same mixes as shown in Figure 3-2.

Total Porosity vs. w/cm ratio for MCU Mixes at 22 °C Cure
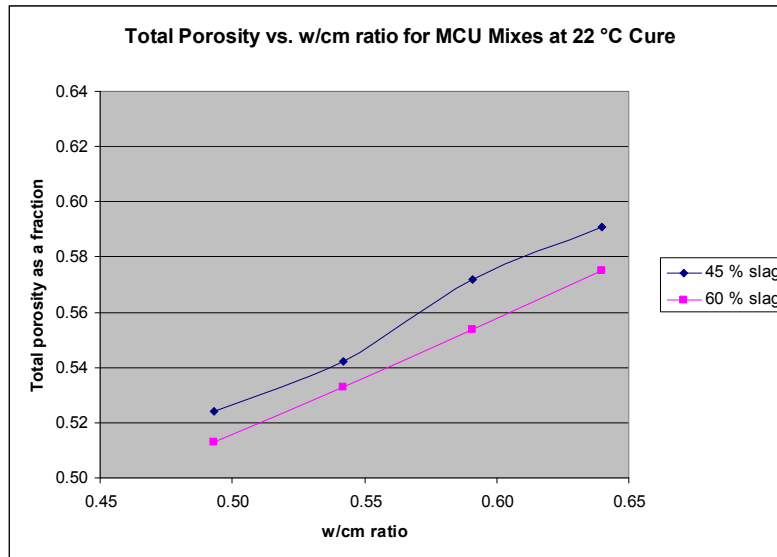
Figure 3-9 Total porosity for mixes batched with either 45 or 60 wt % slag as a function of w/cm ratio. Porosities were measured after 28 days of curing at 22 °C.

Figure 3-10 shows the dependence of total porosity on curing temperature for samples that contain 45 and 60 wt % slag in the premix. The total porosity increases with increasing curing temperature which again, as expected by the inverse relationship between E and porosity, corresponds to the data obtained for Young's modulus over these variables (Figure 3-2). The correlation of E and Φ is discussed in Section 3-11.

Total Porosity vs. Temperature of Curing for 45 wt % BFS

Total Porosity vs. Temperature of Curing at 60 wt % BFS
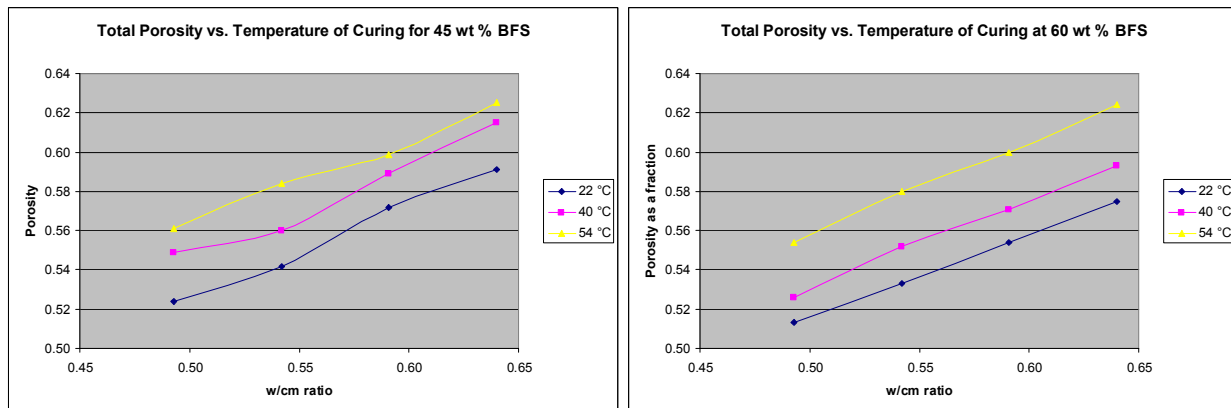
Figure 3-10 Total porosity as a function of w/cm ratio for 3 cure temperatures.

3.5 Heat of Hydration

The heat of hydration data for Phase 10 mixes are provided in Table 3-3. As the w/cm ratio increases for both the 45 and 60 wt % slag mixes, the heat of hydration normalized to the premix

content actually increases slightly except for the w/cm ratio mix of 0.50 for both slag mixes. However, the heat of hydration normalized to the amount of grout is essentially the same for mixes with 45 wt % BFS (~ 110 J/g) and 60 wt % BFS (~ 140 J/g). The difference in heat generation between these two sets is mainly due to the differences in slag content. The empirical model developed and discussed in Section 5 of this report details the dependence of heat of hydration on the significant factors for the combined 10 and 11 phases.

Table 3-3 Heat of Hydration and Peak Time for Heat Generation for Phase 10 Mixes

Identifier	Channel #	Heat of Hydration J/g of premix	Heat of Hydration J/g of grout	Peak time hours
GVS107	6	139	76	4
GVS108	1	211	125	37
GVS109	2	190	107	43
GVS110	3	202	110	48
GVS111	4	210	110	52
GVS112	5	250	147	24
GVS113	6	250	141	29
GVS114	7	258	140	26
GVS115	8	268	135	29

3.6 Electron Microscopy

In an effort to better understand the microstructure of these mixes as a function of temperature, samples were submitted for imaging by Scanning Electron Microscopy (SEM). Figure 3-11 shows the electron micrographs of GVS11 cured at 22 °C and 54 °C. These samples were polished first and then imaged using Back-Scattered Electrons (BSE) with SEM at Clemson University. The top image is for the sample cured at 22 °C and shows individual particles including the spherical fly ash particles. The bottom image in Figure 3-11 was cured at 54 °C and shows a different morphology. Chemical analyses of selected regions were performed by energy dispersive X-ray techniques. These results are preliminary only and have not been duplicated or validated by other samples since funding for this task was stopped after the first set of data was acquired. Nevertheless, the results are revealing, show the power of the technique to characterize these samples, and have the potential to provide insight into the hydration products as a function of curing temperature. It is recommended that additional SEM characterization of the samples as a function of temperature of curing and aluminate concentration in the salt solution be performed in FY10.
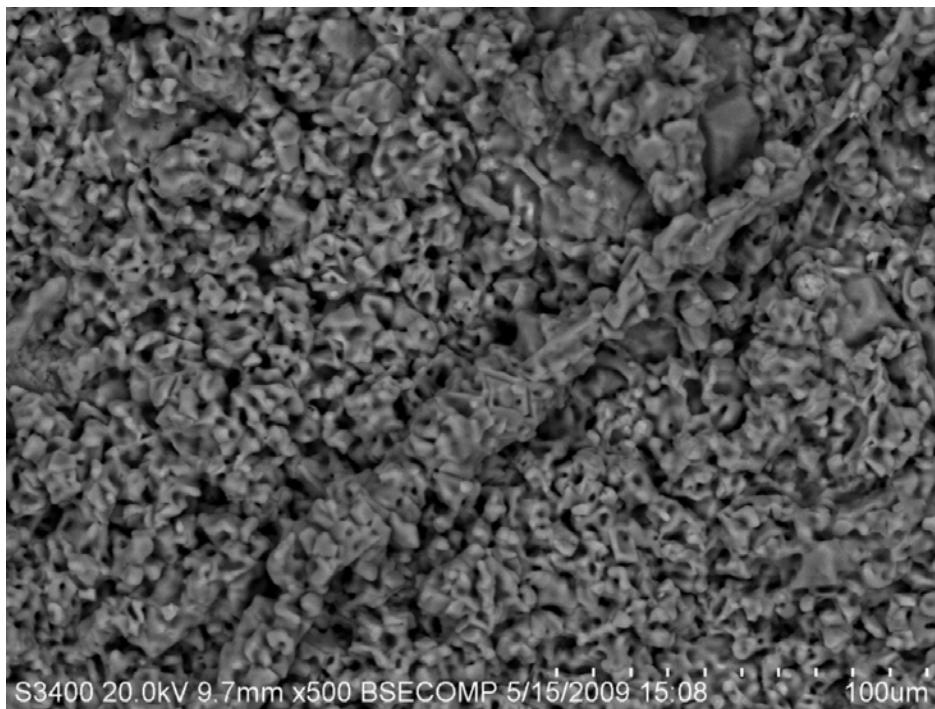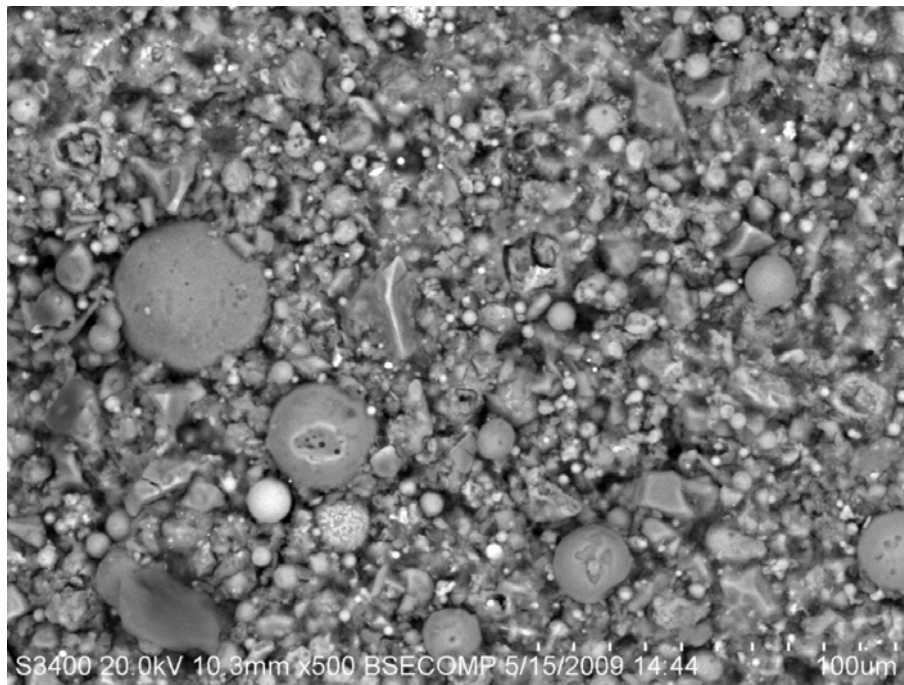
Figure 3-11 BSE micrographs of polished samples of GVS11 cured at 22 °C (top image) and 54 °C (bottom image).

3.7 Processing Properties

Task 3 focused mainly on the performance properties of the ARP/MCU Saltstone mixes. However, the processing properties must also be acceptable for processing at SPF. The processing property results for Phase 10 mixes are presented in Table 3-4. Three of the mixes had gel times reported as 10 minutes (the mixes had gelled at 20 minutes so the real gel time is between 10 and 20 minutes). These short gel times were associated with the 3 mixes at the low w/cm ratios (0.50 and 0.55) and 2 of these 3 mixes had 60 wt % slag content. The lower w/cm ratio mixes also had relatively high yield stress and plastic viscosity values. Acceptance criteria for the flow properties have yet to be established and pumping calculations will be required to determine these criteria. At 22 °C, there was a small amount of bleed on some of the mixes at 1 day but no bleed was evident on any of the mixes at 3 days. For these mixes cured at either 40 °C or 60 °C there was no bleed water at 1 day.   Set times for the 0.22 M aluminate mixes were either 2 or 3 days at 22 °C, and less than 1 day when cured at the higher temperatures.

Table 3-4 Processing Properties for Phase 10 Mixes.

Identifier	Gel Time	Fresh Density	Cured Density	Flow	Uncorrected Yield Stress	Uncorrected Viscosity	1-Day Bleed 22 °C	1-Day Bleed 40 °C	1-Day Bleed 60 °C	3-Day Bleed 22 °C	Set Time 22 °C	Set Time 40 °C	Set Time 60 °C
	minutes	g/mL	g/mL	cm	Pa	cP	Vol %	Vol %	Vol %	Vol %	Days	Days	Days
GVS107	30	1.719	1.753	21.4	6.2	98.4	0.0	0.0	0.0	0.0	1	1	1
GVS108	10	1.791	1.827	18.2	11.0	206.5	0.3	0.0	0.0	0.0	2	1	1
GVS109	20	1.751	1.784	20.9	6.3	125.2	0.4	0.0	0.0	0.0	2	1	1
GVS110	30	1.722	1.750	23.3	4.7	89.5	0.6	0.0	0.0	0.0	3	1	1
GVS111	30	1.710	1.734	25.3	3.0	58.4	0.9	0.8	0.0	0.0	3	1	1
GVS112	10	1.818	1.862	17.7	14.9	213.2	0.0	0.0	0.0	0.0	2	1	1
GVS113	10	1.777	1.831	20.4	8.7	128.9	0.3	0.0	0.0	0.0	2	1	1
GVS114	25	1.744	1.791	23.0	5.7	88.2	0.5	0.0	0.0	0.0	2	1	1
GVS115	20	1.714	1.768	25.0	4.3	64.6	0.5	0.0	0.0	0.0	2	1	1

3.8 Drying Shrinkage and Cracking

Cast samples of GVS107 through GVS115 were removed from the plastic cylinders and placed in an oven at 40 °C for a period of several months. The mass losses due to water evaporation are shown in Figure 3-12.   GVS107 is the only sample with low (0.05 M) aluminate and this sample exhibited a unique mass loss curve relative to the other mixes (with aluminate at 0.22 M). These losses overall are substantial and approach the values of mass loss that have been measured for the porosity tests in which the samples are heated to 105 °C until no further change in mass occurs. The longer times required for mass loss of the cylinders are due to the differences in (1) surface area (the porosity measurements are carried out with a crushed sample) and (2) temperature of drying (40 °C vs. 105 °C).
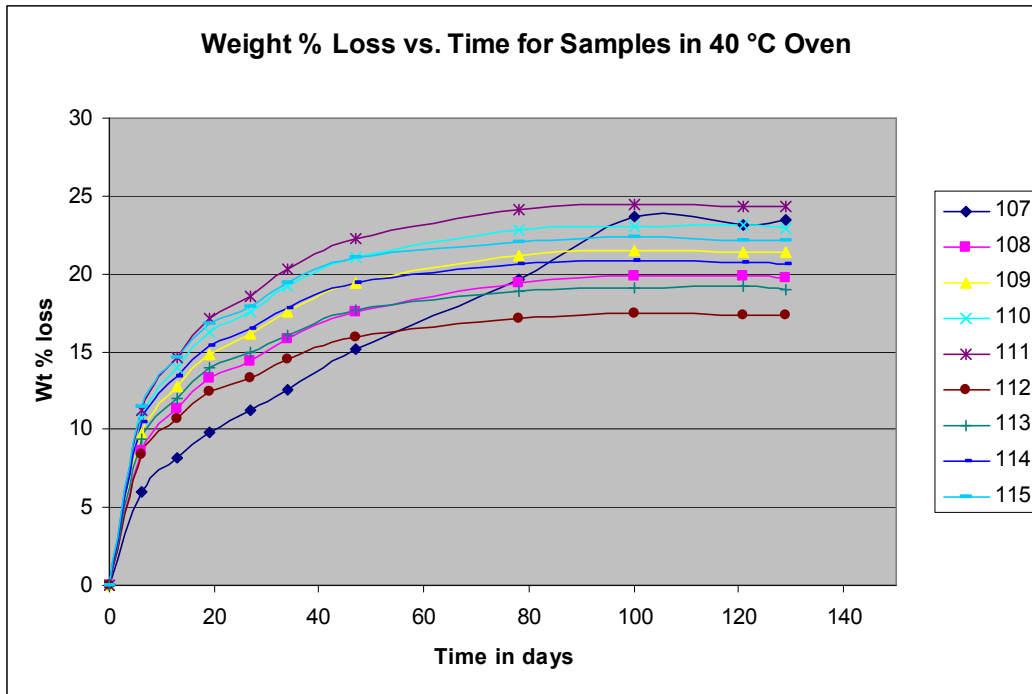
Figure 3-12 Wt % loss of GVS samples numbered 107 through 115 as a function of time in the 40 °C oven.

A photograph of the GVS107 after drying is shown in the left side of Figure 3-13. The photo to the right of this in Figure 3-13 is the sample after being broken by a blow from a hammer. In this case the cylinder broke apart into several large pieces with relatively smooth surfaces. This is in contrast to the other 8 samples of Phase 10 which exhibited a different outcome after being broken.
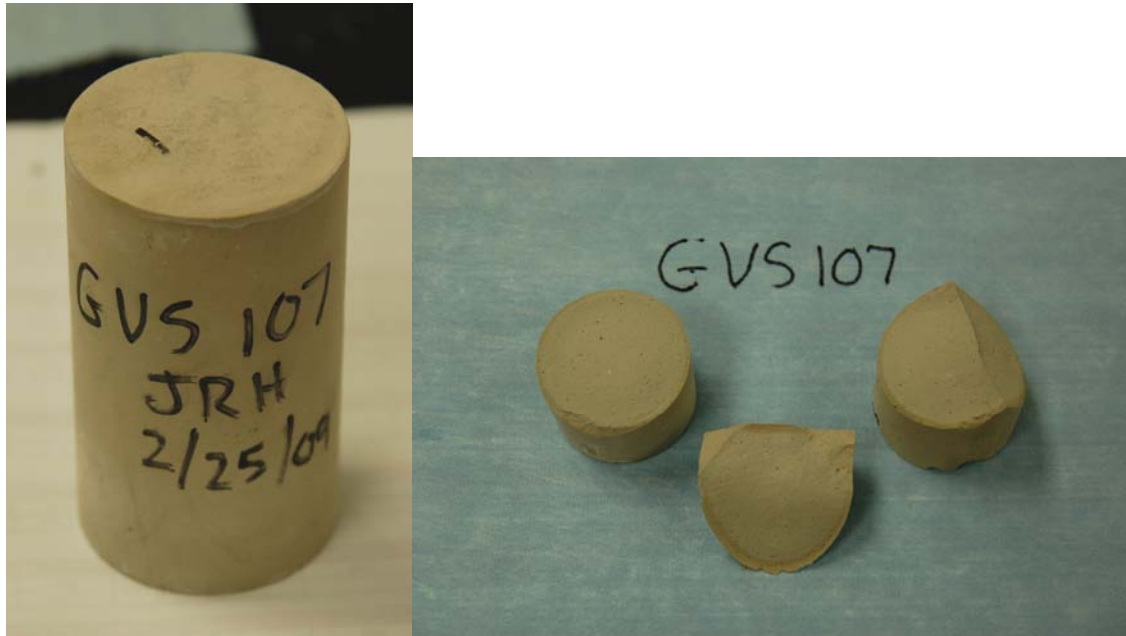
Figure 3-13 GVS107 after drying (image on the left) and then after being broken apart.

The samples from GVS108 through GVS115 showed evidence of surface cracking after drying at 40 °C. The cylinders were broken apart with a hammer which resulted in a crushed material with jagged edges reflective of cleavage along the cracks (Figures 3-14 and 3-15).

Figure 3-14 Cast cylinder of GVS111 after rehydration and cracking.
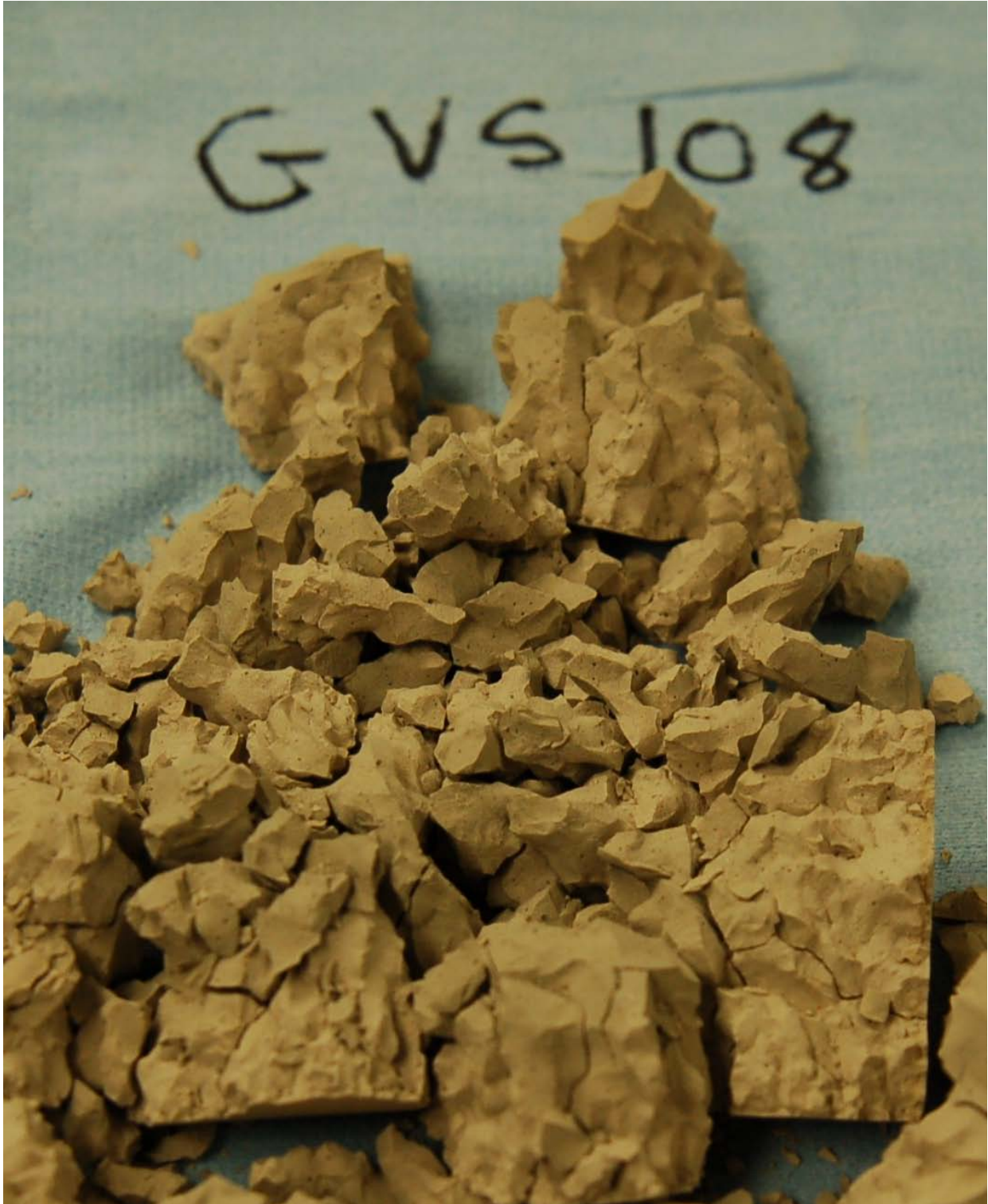
Figure 3-15 Cast cylinder of GVS108 after rehydration and broken apart using a hammer.

Several cured samples were partially dried resulting in a ~ 10 wt % decrease as a result of water loss. Subsequent breaking of these cylindrical samples resulted in a circular cross section that revealed two distinct regions. Figure 3-16 provides an example of a 2 inch diameter cast cylinder that was partially dried and then broken by hand. This example is for a mix containing BFS at 0.60 w/cm ratio in 3.0 M NaOH. There was an inner core that was intact, saturated, and blue in color (typical of samples containing slag) with no evidence of cracking. The outer surface was completely dried, white, and highly cracked as evidenced by the fractured surface. It appears that the samples dry from the outside first which leads to shrinkage and then cracking of the grout as the drying continues. This dried and cracked region is highly permeable such that water from the inner regions escapes from the grout by passing through the porous outer region as drying continues. The kinetics of this process are such that a very sharp demarcation boundary exists between the two phases. The results indicate that drying from the surface of grout can lead to irreversible cracking and increased permeability and porosity in the dried region.

Figure 3-16 A partially dried cured sample (2 inch diameter) from premix and 3.0 M NaOH at 0.60 w/cm ratio and cured at 22 °C. This sample was easily broken by hand.

4.0 RESULTS AND DISCUSSION FOR PHASE 11

Phase 11 used an ARP/MCU simulated salt solution containing 0.22 M aluminate for all the mixes and investigated the impact of increasing the wt % of PC at the expense of FA in the premix. The experimental design is presented in Table 4-1.

Table 4-1 Experimental Design for Phase 11.

Grout Variability Study Phase 11 MCU										
Run Number	Temp	Water/Premix	OPC	FA	Slag	Added OH	Free OH	Nitrate plus Nitrite	Phosphate	Aluminate
Run Order	°C	Ratio	Wt %	Wt %	Wt %	Molarity	Molarity	Molarity	Molarity	Molarity
GVS116	22	0.56	22.5	32.5	45	2.68	1.80	2.91	0.012	0.22
GVS117	22	0.60	15	40	45	2.68	1.80	2.91	0.012	0.22
GVS118	22	0.60	30	25	45	2.68	1.80	2.91	0.012	0.22
GVS119	22	0.52	15	40	45	2.68	1.80	2.91	0.012	0.22
GVS120	22	0.52	30	25	45	2.68	1.80	2.91	0.012	0.22

4.1 Impact of Increased Cement Content in the Mix

A comparison on the impact of an increase in the portland cement wt % in the premix at the expense of the fly ash on the ARP/MCU mix properties can be made using two mixes that were identical except for the wt % portland cement concentration (10 wt % for GVS110 vs. 30 wt % for GVS118). GVS110 is the baseline mix at 0.60 w/cm ratio with a salt stream composition projected by Thuy Le.

The fresh and cured grout properties of these two mixes are presented in Table 4-2. The set time is reduced to 1 day at 22 °C for the higher cement mix consistent with the shorter induction period of 3 hours versus the 48 hours for the GVS110 mix. The gel time is reduced to 5 minutes with 30 wt % cement and the yield stress and plastic viscosity also increase as a result of increased cement. Although the heat of hydration is greater in GVS118, the values of E are less than the corresponding value with the baseline mix. On the other hand, the porosities for the two mixes are roughly the same. This effect of improved permeability and Young's modulus has been reported in the literature for mixes containing higher ratios of slag to cement [9]. This difference in performance properties for mixes containing a higher proportion of cement leads to difficulty in the predictive models (see Section 6).

Table 4-2 Fresh and Cured Grout Properties for GVS110 and GVS118

Identifier	Gel Time	Fresh Density	Cured Density	Flow	Yield Stress	Viscosity	Bleed	Set Time
	minutes	g/mL	g/mL	cm	Pa	cP	Vol %	Days
GVS110	30	1.722	1.750	23.3	4.7	89.5	0.5	3.0
GVS118	5	1.761	1.796	19.7	6.9	116.1	0.0	1.0

	Porosity	Heat	E
	Volume %	J/g cm	GPa
GVS110	57.2	202.0	8.8
GVS118	56.8	239.0	7.2

4.2 Phase 11 – E as a Function of w/cm Ratio and Wt % Cement

The values of Young's moduli for the five ARP/MCU mixes for Phase 11 as a function of w/cm ratio at two different cement loadings are presented in Table 4-3. The baseline ARP/MCU mix, GVS110, from Phase 10 is also included for reference. The Phase 11 samples were cured under sealed conditions at room temperature (22 °C).

Table 4-3 Young's Modulus Values for the Phase 11 Mixes.

Young's Modulus in GPa after 31 Days			
	22 °C	40 °C	60 °C
GVS110	8.8	7.2	4.5
GVS116	7.7	6.6	6.4
GVS117	8.0	5.9	4.4
GVS118	7.2	6.5	6.8
GVS119	9.0	7.0	5.9
GVS120	8.6	8.0	8.4

An increase in cement concentration in the premix from 10 wt % to 15 wt % to 30 wt % reduces E for samples cured at 22 °C for a w/cm ratio of 0.60 (Figure 4-1). Reducing the w/cm ratio from 0.60 to 0.52 at 22 °C increases Young's modulus at the same premix composition. On the other hand, samples with higher cement content that are cured at either 40 °C or 60 °C show improvement in E over the baseline mix at these curing temperatures. In fact, the mixes containing 30 wt % cement in the premix (GVS118 and GVS120) have E values that are relatively insensitive to the temperature of curing (Table 4-3). The mixes with lower levels of cement show greater reduction in E at higher curing temperatures, a response that is typical of mixes with the nominal premix composition.
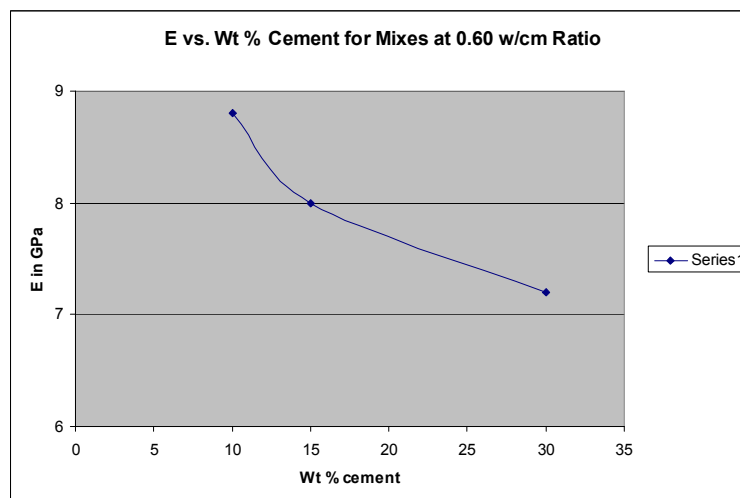
Figure 4-1 E vs. wt % cement in baseline ARP/MCU mix for samples cured at 22 °C.

The time dependence of E for a curing temperature of 22 °C is given in Figure 4-2 for each of the 5 mixes of Phase 11 plus GVS110 from Phase 10 (brown-colored curve). Relative to the baseline ARP/MCU mix (GVS110), these samples show a greater increase in E with time out to measurements at 91 days.
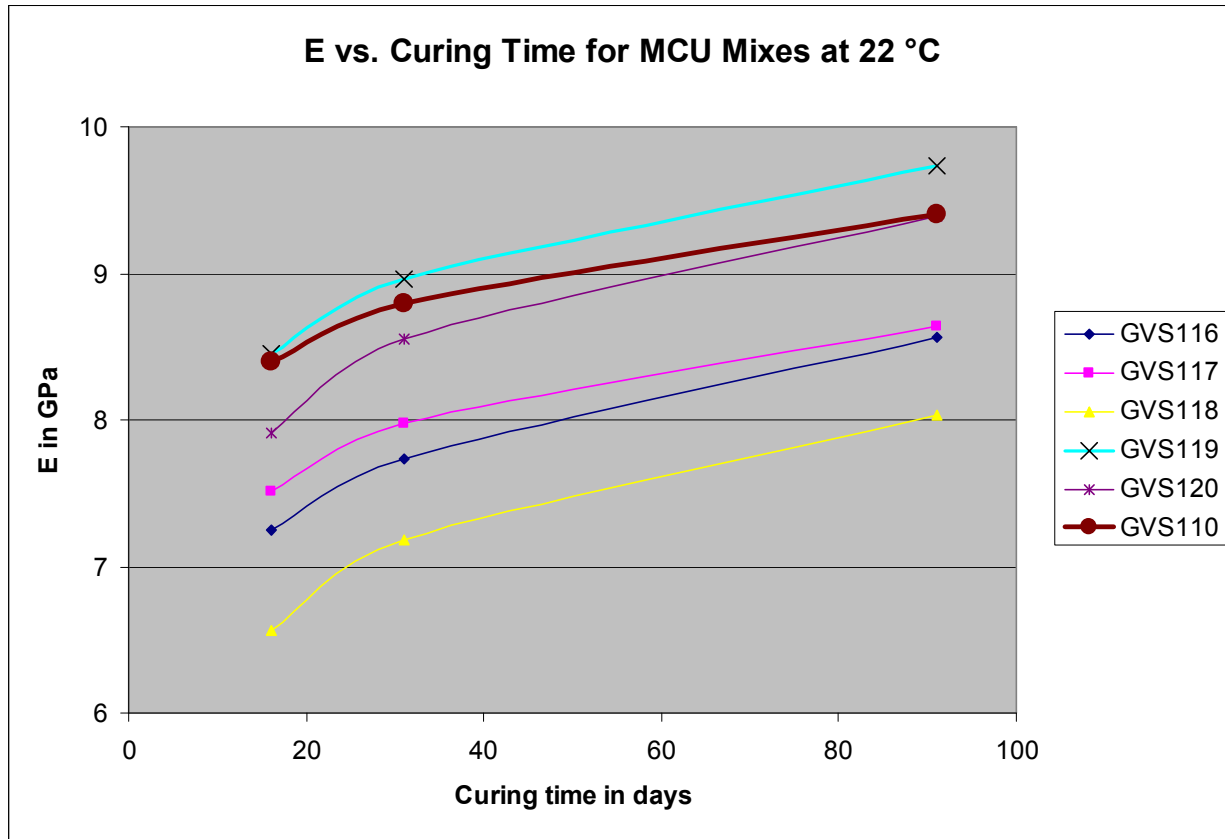
Figure 4-2 Time dependence of E at 22 °C curing temperature for the five mixes of Phase 11 plus GVS110 from Phase 10.

4.3 Young's Modulus at Different Time/Temperature Curing Profiles

Previous results [4] have shown that the performance properties of the mixes depend on the time/temperature profile for curing. Figure 4-3 shows the dependence of E on time and temperature curing profiles for a mix at 0.60 w/cm ratio (GVS118) with a cement concentration of 30 wt % of the premix. The time/temperature curing profile for each curve is provided in the table below the figure. The data show that an increase in temperature to 60 °C after 1 or 2 days curing at 22 °C does not significantly reduce E. This is in contrast to the previous results of this report for a mix containing the nominal premix distribution (Section 3-3). For mixes cured initially at 60 °C, removal after 1 or 2 days at 60 °C followed by curing at 22 °C, results in mixes with lower E values than the mix cured for 7 days at 60 °C. This pattern is consistent with mixes batched with the nominal premix distribution (Section 3-3).

.

E as a Function of Time for Phase 11 Mix GVS118
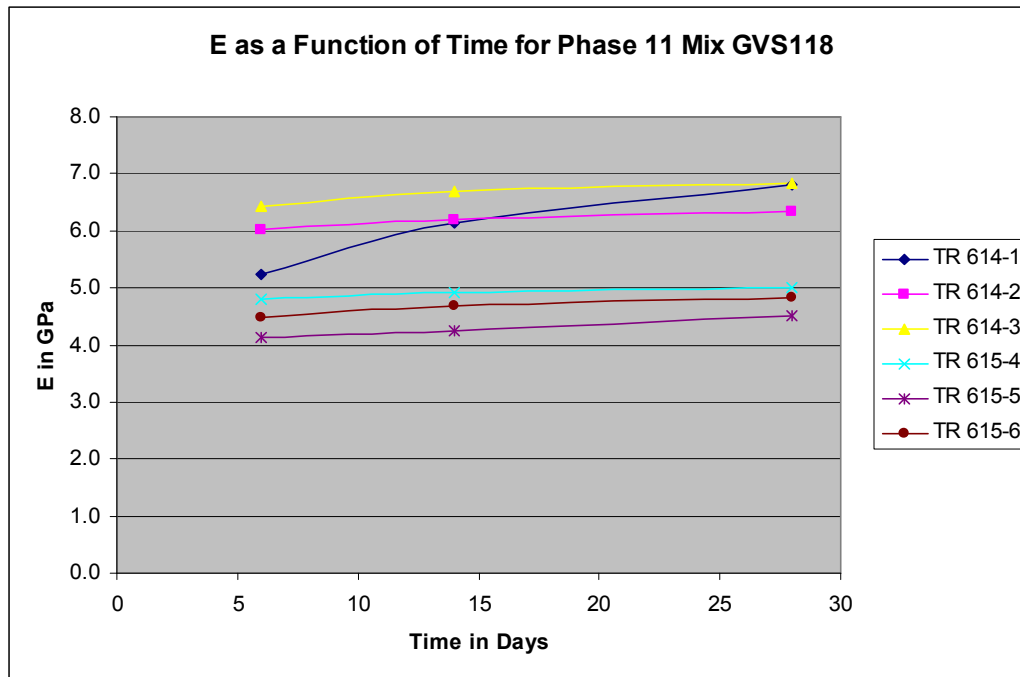
TR #	Time/ Temperature Profile	TR #	Time/ Temperature Profile
TR 614-1	Curing only at 22 °C	TR 615-4	7 days at 60 °C
TR 614-2	1 day at 22 °C and 6 days at 60 °C	TR 615-5	1 day at 60 °C and 6 days at 22 °C
TR 614-3	2 days at 22 °C and 5 days at 60 °C	TR 615-6	2 days at 60 °C and 5 days at 22 °C

Figure 4-3 E as a function of curing time for the profiles given in the legend for GVS118.

4.4 Porosities as a Function of Curing Temperature and Time

The total porosity values for the Phase 11 mixes along with the baseline mix (GVS110) are provided in Table 4-4. For samples cured at 22 °C, Φ decreases with w/cm ratio but is independent of the cement concentration. These porosities are also less than Φ for the baseline mix. The porosities decrease for samples cured at either 40 °C or 60 °C relative to 22 °C for all of the mixes except those containing 30 wt % cement. For the high cement mixes, the porosities are essentially independent of the curing temperature and consistent with the trend of Young's moduli which were also independent of curing temperature.

Table 4-4 Total Porosity Values for the Phase 11 Mixes.

Total Porosity after 31 days			
	22 °C	40 °C	60 °C
GVS110	0.572	0.589	0.599
GVS116	0.552	0.567	0.580
GVS117	0.567	0.591	0.591
GVS118	0.568	0.571	0.561
GVS119	0.538	0.559	0.561
GVS120	0.535	0.536	0.526

4.5 Heat of Hydration

The heat of hydration data for Phase 11 mixes are provided in Table 4-5. As the w/cm ratio increases for both the 15 and 30 wt % cement mixes, the heat of hydration normalized to the premix content actually increases slightly. As the PC content is increased from 15 to 30 wt %, the normalized heat of hydration also increases. However, a reduction in w/cm ratio from 0.60 to 0.52 reduces the J/g of premix produced over the same time period. Higher cement content at either w/cm ratio shortens the peak time for heat generation. The model produced and discussed in Section 5 of this report details the dependence of heat of hydration on the significant factors for the combination of Phase 10 and 11 mixes.

Table 4-5 Heat of Hydration and Peak Time for Heat Generation for Phase 11 Mixes.

Identifier	Channel #	Heat of Hydration	Heat of Hydration	Peak time
		J/g of premix	J/g of grout	hours
GVS116	1	211	118	6
GVS117	2	208	112	11
GVS118	3	239	129	3
GVS119	4	192	109	22
GVS120	5	221	127	4

4.6 Processing Properties for Phase 11 Mixes

Task 3 focused mainly on the performance properties of the ARP/MCU Saltstone mixes. However, the processing properties must also be acceptable for processing at SPF. The processing property results for Phase 11 mixes are presented in Table 4-6. Almost all of the mixes had gel times that were less than 20 minutes. Therefore, a set retarder may be required if a premix with higher levels of cement were used at Saltstone. The mixes had relatively high yield stress and plastic viscosity values with the higher cement content. Acceptance criteria for the flow properties have yet to be established and pumping calculations will be required to determine

these criteria. There was no bleed on any of the samples and the set time was 1 day for all the mixes except GVS117 in spite of the fact that these mixes had relatively high aluminate levels. This suggests that a larger concentration of portland cement in the premix accelerates the set. For these mixes cured at either 40 °C or 60 °C there was no bleed water at 1 day.

Table 4-6 Processing Properties for Phase 11 Mixes.

Identifier	Gel Time	Fresh Density	Cured Density	Flow	Uncorrected Yield Stress	Viscosity	1-Day Bleed 22 °C	40 °C	60 °C	3-Day Bleed 22 °C	Set Time 22 °C	40 °C	60 °C
	minutes	g/mL	g/mL	cm	Pa	cP	Vol %	Vol %	Vol %	Vol %	Days	Days	Days
GVS116	5	1.772	1.796	20.1	10.4	139.0	0.0	0.0	0.0	0.0	1	1	1
GVS117	20	1.728	1.761	23.5	4.0	76.6	0.4	0.5	0.0	0.0	2	1	1
GVS118	5	1.761	1.796	19.7	6.9	116.1	0.0	0.0	0.0	0.0	1	1	1
GVS119	10	1.789	1.823	20.3	7.9	141.8	0.0	0.0	0.0	0.0	1	1	1
GVS120	5	1.843	1.865	17.5	15.8	206.3	0.0	0.0	0.0	0.0	1	1	1

4.7 Drying Shrinkage and Cracking

Cast samples of GVS116 through GVS120 were placed in a 40 °C oven and weighed periodically to determine the rate of water loss from the 2 x 4 inch cylinders. The time dependence of this mass loss is shown in Figure 4-4. The loss in wt % is in expected order with higher water loss observed for those samples having higher w/cm ratios and lower water loss for those samples containing higher concentrations of portland cement.

Figure 4-5 shows a plot of mass loss at 40 °C versus the mass loss at 105 °C for these five samples. This plot shows that the mass loss at 105 °C is ~ 22 % greater than the mass loss at 40 °C for all of the samples.
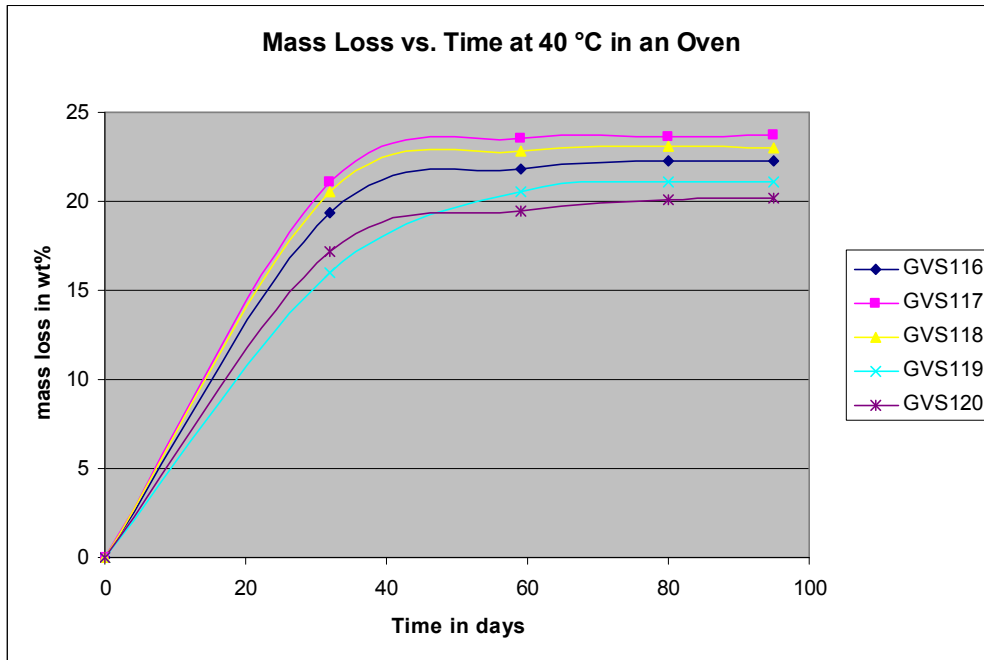
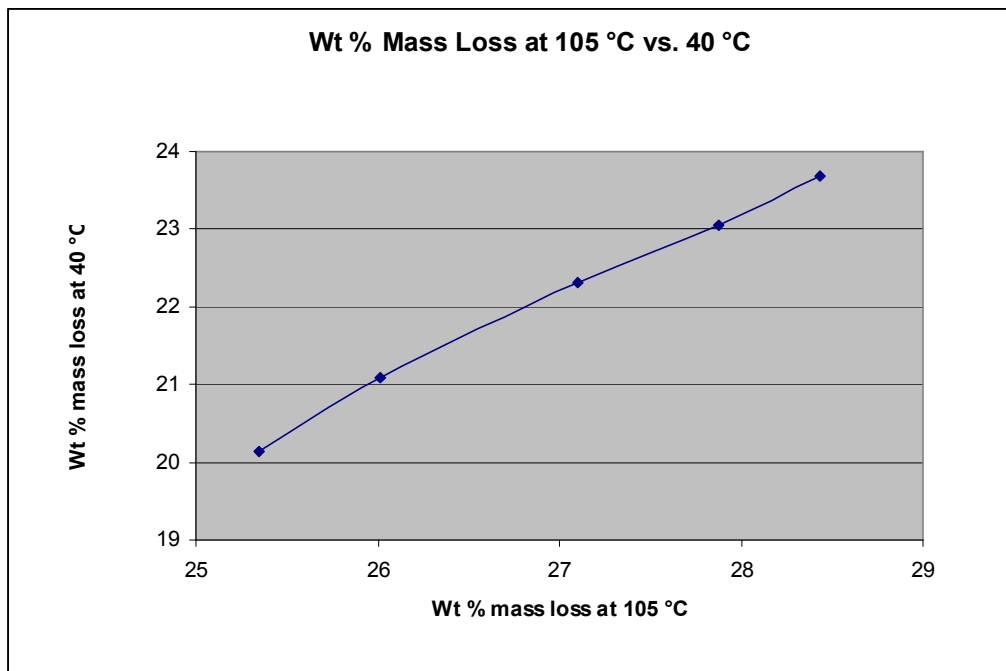**Figure 4-4 Mass loss in wt % for the 2 x 4 inch cast samples of GVS116 through GVS120.**

Figure 4-5 A comparison of mass loss in wt % for drying at 40 °C vs. 105 °C for the 2 x 4 inch cast samples of GVS116 through GVS120.

Figure 4-6 provides a photograph of GVS120 after drying and rehydration. Before breakage, surface cracks are evident in this photo (image on the left). An image of the cross section of this cast cylinder after breakage by hand into two pieces is shown on the right side of this figure. The surface consists of jagged edges reflective of cleavage along the cracks. These results were similar to those seen for samples dried and broken from Phase 10 of this task (with high aluminate in the salt feed).

Figure 4-6 Photographs of GVS120 after drying and rehydration (left side) and breakage (right side).

5.0 CORRELATION OF POROSITY AND YOUNG'S MODULUS

Figure 5-1 is the plot of Young's modulus (E) versus total porosity (Φ) for all of the mixes of Phases 10 and 11 cured at 22 °C [11]. Phase 10 data are designated by gold squares whereas phase 11 samples are designated by purple filled circles.   It is clear from this figure that phase makes a difference in the correlation. The offset reflects the incorporation of higher concentrations of cement in the Phase 11 samples. As indicated earlier in this report, the use of slag at the expense of cement in mixes improves permeability and presumably Young's modulus. Since cement was increased at the expense of fly ash, the impact of reduced fly ash concentration in the premix also has to be considered. Fly ash is also known to improve permeability. Therefore, both the increase in cement and decrease in fly ash concentrations result in a mix with lower E values. One approach to dealing with this property is to correlate only over a similar type of premix. The changes in cement and fly ash in the Phase 11 mixes is larger than would be normally expected for operational variation of these concentrations at the SPF. Therefore, for a given batch, a unique correlation may be determined that is appropriate for the premix composition selected.
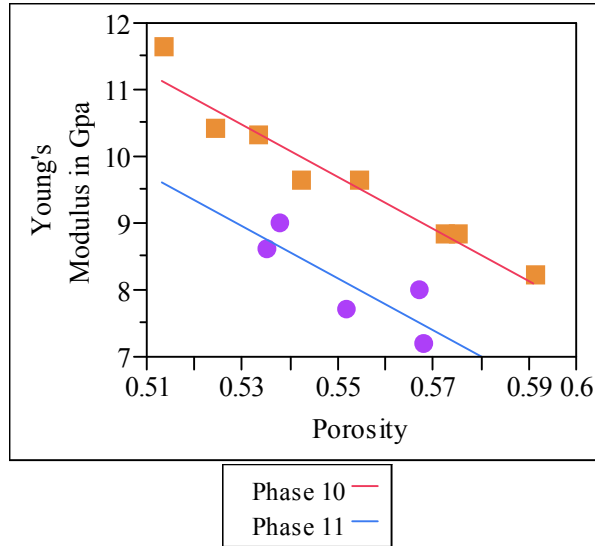
Figure 5-1 Correlation of E and Φ for Phases 10 and 11 mixes cured at 22 °C. The purple circles are Phase 11 mixes and the gold squares are Phase 10 mixes.

When results of E and Φ from all the mixes at all three curing temperatures are plotted, the result shown in Figure 5-2 is obtained with a higher degree of scatter as reflected in an R^2 of 67 %. The difference in correlation between the two phases is still evident. The linear correlation based on all of the results is represented by the following equation:

$$E \text{ (GPa)} = 38.22757 - 54.220437 * \Phi$$
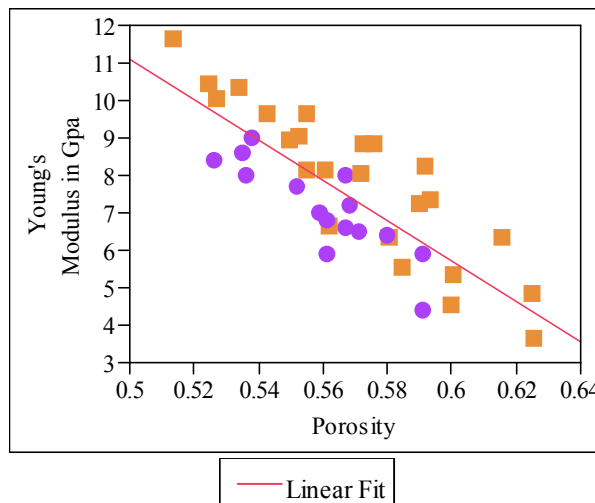
Figure 5-2 Bivariate fit of Young's modulus to total porosity for mixes of Phases 10 and 11 measured at all three curing temperatures. The purple circles are Phase 11 mixes and the gold squares are Phase 10 mixes.

6.0 PREDICTIVE MODELING FOR E, Φ AND HEAT OF HYDRATION

One of the goals of this work was to identify the factors that drive the values of physical properties (responses) of the Saltstone mixes. In this section of the report, the results of models developed using JMP Version 7.02 [11] for Young's modulus, total porosity and heat of hydration are presented. The results using only samples cured at 22 °C will be presented first and then the results using samples cured at all three temperatures will be presented.

For Young's modulus, the predicted versus actual values are plotted and provide a linear fit with an R^2 equal to 95 % (Figure 6-1).   These data points are for Phases 10 and 11 for the mixes cured at 22 °C.
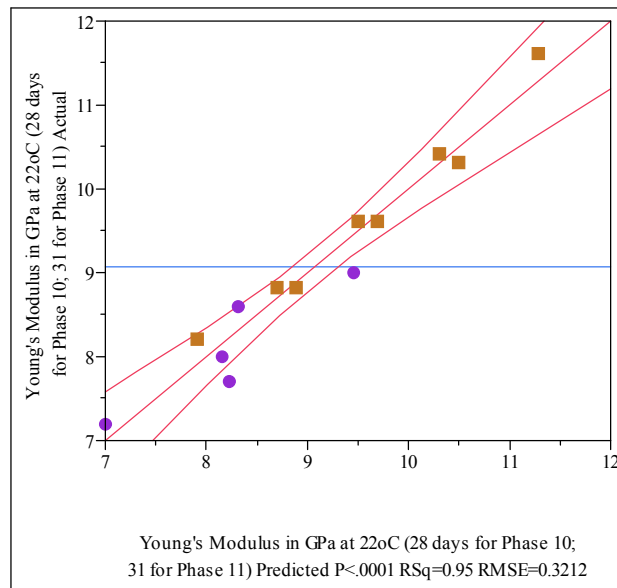
Figure 6-1 Actual versus predicted values of Young's modulus for samples of Phases 10 and 11 for samples cured at 22 °C.

The model (equation) for prediction of E is:

E = 16.1 – 16.3•w/cm + 0.07•wt % slag – 0.08•wt % cement

For total porosity, the predicted versus actual values are plotted and provide a linear fit with an R^2 equal to 99 % (Figure 6-2).   These data points are for Phases 10 and 11 for the mixes cured at 22 °C.
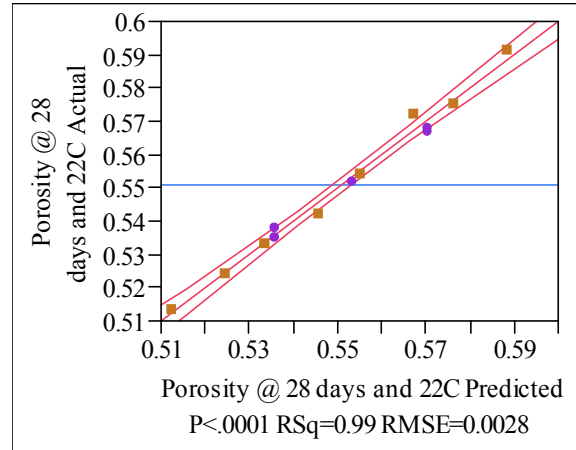
Figure 6-2 Actual vs. predicted values of total porosity for samples of Phases 10 and 11 for samples cured at 22 °C.

The model (with an R^2 of 99 %) for prediction of total porosity (Φ) expressed as a fraction is:

Φ = 0.35 + 0.44•w/cm - 0.001•wt % slag

The heat of hydration in J/g of cm was also modeled and the results are provided in Figure 6-3.

Figure 6-3 Actual vs. predicted values of heat of hydration for samples of Phases 10 and 11 for samples cured 25 °C only.

The model (equation) for prediction of heat of hydration (HOH) expressed in J/g of cm is:

HOH = 94.2 + 104.4•w/cm + 2.4•wt % slag – 1.4•wt % FA

The R^2 for this fit is 92% and identifies w/cm ratio, wt % slag and wt % FA as the significant drivers of the heat of hydration of the Saltstone mixes.

The predicted versus actual values for Young's modulus for Phases 10 and 11 mixes cured at three different temperatures are plotted in Figure 6-4.

Figure 6-4 Actual versus predicted values of Young's modulus for samples of Phases 10 and 11 for samples cured at all three temperatures.

The model (with an R^2 of 80 %) for prediction of E, where T is the temperature in °C, is:

E = 17.9 – 18.3•w/cm + 0.07•wt % slag - 0.09•T

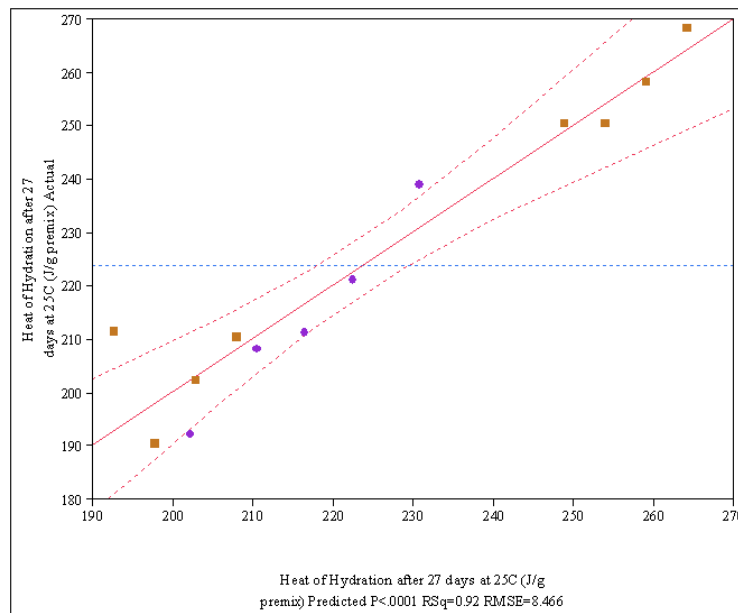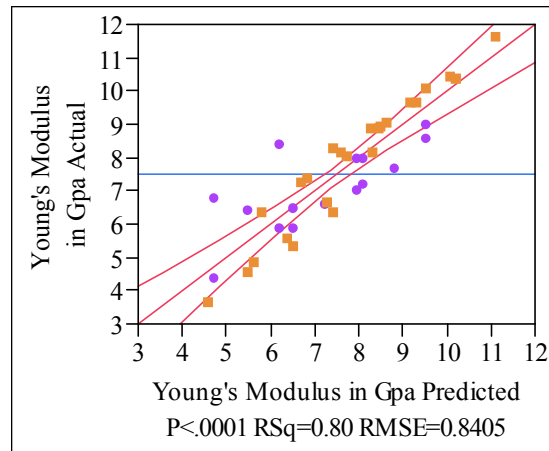The predicted versus actual values for total porosity for Phases 10 and 11 mixes cured at three different temperatures are plotted in Figure 6-5.
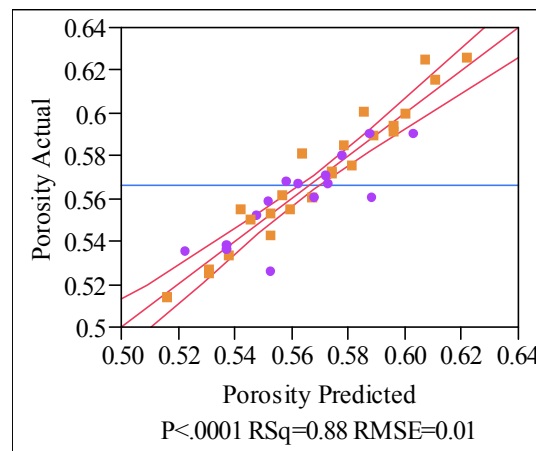

Figure 6-5 Actual vs. predicted values of total porosity for samples of Phases 10 and 11 for samples cured at all three temperatures.

The model (with an R^2 of 88 %) for prediction of Φ, where T is the temperature in °C, is:

$$\Phi = 0.25 + 0.44 \cdot w/cm + 0.001 \cdot wt\ \%\ FA + 0.0008 \cdot T$$

There are two mixes that have porosities and E values that are not well predicted by the models. These are the mixes containing 30 wt % cement cured at 60 °C (GVS118 and GVS120). As discussed previously, this additional cement concentration does not follow the normal reduction in E and increase in Φ that are normally seen as the curing temperature is raised. Therefore, the system is no longer typical of the normal or close to normal premix composition currently used at SPF. Excluding these extreme premix compositions from the model will increase R^2 and provide a better predictive equation.

A similar lack of predictability is seen with a difference in the aluminate concentration in the salt solution. GVS107 results were not included in the modeling since it had an aluminate concentration that was very low compared to the projections (0.05 vs. 0.22 M). Nevertheless this 0.05 M aluminate mix does provide a reference point for understanding the impact of aluminate. With aluminate at this level, E is much lower and Φ is much higher than predicted by the models presented in this report. Therefore, the compositional region of the salt solution over which variation is introduced to develop models is extremely important for development of quality models.

7.0 CONCLUSIONS

Task 3 of the FY09 Variability Study focused on the performance (but also measured the processing) properties of Saltstone mixes batched using the projected ARP/MCU decontaminated salt solutions (an average of Batches ISDP3-5). The major conclusions of this task are:

- The relatively high 0.22 M aluminate concentration in the projected ARP/MCU batches significantly increased Young's modulus compared to the previous baseline ARP/MCU composition with 0.05 M aluminate for curing at 22 °C (E more than doubled from 4.2 to 8.8 GPa).
- The total porosity decreased from 59.1 % to 57.2 % from the 0.05 M to the 0.22 M aluminate mixes. Both the increase in E and reduction in Φ lead to improved performance for samples cured at 22 °C.
- For the baseline ARP/MCU mix with 0.22 M aluminate and cured at 22 °C, a decrease in the w/cm ratio increased E and reduced Φ. For the nominal premix composition the results were an increase in E from 8.2 to 10.4 GPa as w/cm ratio decreased from 0.65 to 0.50. Φ decreased from 59.1% to 52.4 % over this same range of w/cm ratio.
- For the baseline ARP/MCU mix with 0.22 M aluminate and cured at 22 °C, an increase in the slag content (at the expense of fly ash) in the premix from 45 to 60 wt % wt % increased E and reduced Φ. E increased ~ 8 % while Φ decreased ~2–3 % for a slag increase from 45 to 60 wt %. Therefore, an increase in slag concentration in the premix improves performance properties.
- For the baseline ARP/MCU mix with 0.22 M aluminate and cured at 22 °C, an increase in the cement content in the premix from 10 to 30 wt % decreased E from 8.8 to 7.2 GPa. This is opposite of the effect of increased slag concentration in the premix.
- For the baseline ARP/MCU mix with 0.22 M aluminate and cured at 22 °C, a decrease in the w/cm ratio for either the 15 or 30 wt % cement mixes increased E and decreased Φ.
- Increasing the temperature of curing for the Phase 10 mixes generally decreased E and increased Φ. However, increasing the temperature of curing for the mixes of Phase 11 with higher cement concentrations revealed that E and Φ were not as sensitive to (i.e., did not decrease in value) the temperature of curing as compared to mixes using the normal premix.
- The sequence of time and temperature of curing again played a major role in the final performance properties of the phase 10 mixes. This effect was mitigated for the Phase 11 mixes containing higher cement levels.
- For the Phase 10 mixes, the processing properties were generally acceptable except for those mixes at low w/cm ratios. The measured gel times for these mixes were 10 minutes and the viscosities and yield strengths were higher than normal. Similar results were found for the Phase 11 mixes where high levels of cement produced short gel times.
- Drying tests were performed for all of the mixes from Phases 10 and 11 at 40 °C. Over the period of one to two months, the mass loss due to water evaporation approached 20 wt %.

- The dried samples when broken apart revealed smaller pieces with surfaces consisting of jagged edges reflective of cleavage along the cracks. This behavior was observed with samples containing 0.22 M aluminate. For the 0.05 M aluminate mix, this behavior was not observed and the cylinder broke apart into several large pieces with relatively smooth surfaces. The preliminary conclusion is that aluminate produces a microstructure that is susceptible to cracking.

- Partially dried samples (< 10 wt % loss), when broken apart revealed distinct cross sectional regions. The outer region was highly fractured whereas the inner region was blue in color, saturated and intact.

- The mechanism leading to this observation is drying shrinkage and subsequent cracking. Evidently the samples dry from the outside first which leads to shrinkage and then cracking of the grout as the drying continues. This dried and cracked region is highly permeable such that water from the inner regions escapes from the grout by passing through the porous outer region. The kinetics of this process are such that a very sharp demarcation boundary exists between the two phases.

- Correlations of E with Φ reveal that Phase 10 mixes produce a curve which is parallel but offset from the curve for Phase 11 mixes. This is due to the fact that cement and slag produce mixes with different values of E and Φ for the same degree of hydration. Slag in general produces a grout with higher E, lower Φ, and lower permeability.

- Linear models were developed relating performance properties to the experimental factors for the mixes cured at 22 °C. The models have high R^2 values and identify the key factors that drive the values of E, Φ and heat of hydration. However, the same predictive models produce more scatter when the results for samples cured at all temperatures are included. The outliers in these plots are the mixes with 30 wt % cement cured at 60 °C which as described above reflects differences in response between cement and slag. The next generation of models may exclude these mixes with high values of cement since they may not be applicable to processing at SPF.

8.0 PATH FORWARD

The results in this report indicate that in order to meaningfully measure the performance properties of Saltstone, one has to know the time/temperature profile conditions under which the Saltstone will be cured. This will require thermal modeling and/or actual time/temperature profiles within the vaults under various pour schedules to determine (1) an average profile of time and temperature under normal processing and (2) a conservative (worst case) profile. Samples can then be cast and cured in the laboratory under these time and temperature profiles prior to measurement of the performance properties of the product waste forms.

This study reveals that drying of the Saltstone, even at relatively low temperatures (e.g., 40 C) can result in shrinkage and subsequent irreversible cracking. It is recommended that the factors that drive this shrinkage be identified and a strategy proposed to mitigate this process.

The role of aluminate and curing temperature as significant drivers of the performance properties suggests that these factors bring about microstructural changes. It is therefore suggested that the microstructure of these samples be investigated by scanning electron microscopy in order to better understand the changes that occur (and consequently, provide a basis for mitigation strategies) as a function of (1) aluminate concentration in the salt solution and (2) curing temperature.

9.0 REFERENCES

[1]   *Memo Report on the Subtasks for the Saltstone Variability Study for 2009*, J. R. Harbour and T. B. Edwards, SRNL L3100-2008-00048, October 2008.

[2]   *Future ISDP Batches to Saltstone Processing Facility, Projected Batch and Key Components Compositions,* T. A. Le, LWO-LWP-2009-00005, Rev. 1, 2009.

[3]   *Effect of Increased Aluminate Concentrations on Saltstone Mixes,* J. R. Harbour, T. B. Edwards, E. K. Hansen and V. J. Williams, WSRC-STI-2007-00506, Rev. 0, 2007.

[4]   *Impact of Time/Temperature Curing Conditions and Aluminate Concentration on Saltstone Properties,* J. R. Harbour, T. B. Edwards and V. J. Williams, SRNL-STI-2009-00184, Rev. 0, 2009.

[5]   *Heat of Hydration of Saltstone Mixes – Measurement by Isothermal Calorimetry*, J. R. Harbour, V. J. Williams and T. B. Edwards, WSRC-STI-2007-00263, Rev. 0, 2007.

[6]   *Saltstone Performance Indicator*, J. R. Harbour and V. J. Williams, SRNL-STI-2008-00488, Rev. 0, December 2008.

[7]   *Saltstone Variability Study –Measurement of Porosity,* J.R. Harbour, V.J. Williams, T.B. Edwards, R.E. Eibling, and R.F. Schumacher, WSRC-STI-2007-00352, Rev. 0.

[8]   *Variability Study for Saltstone*, J. R. Harbour, T. B. Edwards, E. K. Hansen and V. J. Williams, WSRC-TR-2005-00447, October 2005.

[9]   *Cement Chemistry*, H. F. W. Taylor, Thomas Telford Publishing, 1997.

[10]   *Permeability of Saltstone*, J. R. Harbour, T. B. Edwards, V. J. Williams, D. M. Feliciano and G. W. Scherer WSRC-STI-2007-00437, Rev. 0, 2007.

[11]   JMP Version 7.0.2, SAS Institute, Inc. Cary, NC, 1989-2007